Department of Applied Physics

Towards metal free counter electrodes for dye sensitized solar cells

Syed Ghufran Hashmi

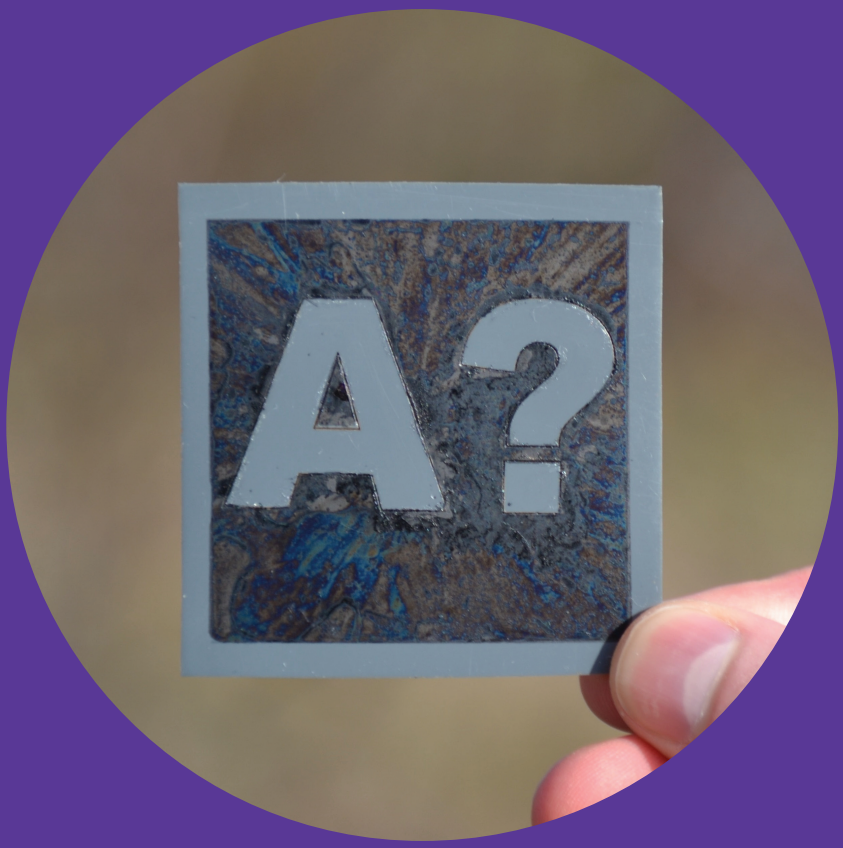

Aalto University

DOCTORAL DISSERTATIONS

Aalto University publication series
DOCTORAL DISSERTATIONS 41/2014

Towards metal free counter electrodes for dye-sensitized solar cells

Syed Ghufran Hashmi

A doctoral dissertation completed for the degree of Doctor of Science (Technology) to be defended, with the permission of the Aalto University School of Science, at a public examination held at the lecture hall 216 of the school on 16 May 2014 at 10:00 am.

Aalto University
School of Science
Department of Applied Physics
New Energy Technologies Group (NEW)

Supervising professor
Professor Peter Lund

Thesis advisor
Dr Janne Halme, Dr Kati Miettunen

Preliminary examiners
Professor Jouko Korppi-Tommola, University of Jyväskylä, Finland.

Professor Helge Lemmetyinen, Tampere University of Technology, Finland.

Opponent
Professor Tingli Ma, Kyushu Institute of Technology, Japan.

Aalto University publication series
DOCTORAL DISSERTATIONS 41/2014

ISBN 978-952-60-5625-8
ISBN 978-952-60-5626-5 (pdf)
ISSN-L 1799-4934
ISSN 1799-4934 (printed)
ISSN 1799-4942 (pdf)
http://urn.fi/URN:ISBN:978-952-60-5626-5

Unigrafia Oy
Helsinki 2014

Finland

441 697
Printed matter

Author
Syed Ghufran Hashmi

Name of the doctoral dissertation
Towards metal free counter electrodes for dye-sensitized solar cells

Publisher School of Science

Unit Department of Applied Physics

Series Aalto University publication series DOCTORAL DISSERTATIONS 41/2014

Field of research Photovoltaics, Micro and nanotechnology, Renewable energy

Manuscript submitted 17 January 2014 **Date of the defence** 16 May 2014

Permission to publish granted (date) 11 March 2014 **Language** English

☐ **Monograph** ☒ **Article dissertation (summary + original articles)**

Abstract

This thesis provides a technical overview of results from addressing the critical steps in preparing counter electrodes for dye-sensitized solar cells (DSC) on flexible substrates (mainly plastics) to pave the way towards low-cost DSCs. The aim was to develop low-temperature counter electrode inks and pastes that could be suitable for high volume manufacturing processes. A special focus was given on the mechanical stability (flexibility and adhesion) of the materials that were deposited through a low-temperature route.

Different low temperature inks and pastes based on carbon composites were tested as a replacement to expensive platinum nanoparticles based catalyst layer and showed good mechanical stability, comparable photovoltaic performance and low charge transfer resistance in complete dye-sensitized solar cells.

Indium doped tin oxide (ITO) layer that is normally used as a conductor on plastic substrates was successfully replaced with a single walled carbon nanotube (SWCNT) film deposited as a low-temperature curable ink on polyvinyl chloride (PVC) substrate. The SWCNT films exhibited remarkably good mechanical stability when subjected to bending and tape adhesion tests. Coating the film with a thin layer of conducting polymer poly (3, 4-ethylenedioxythiophene (PEDOT) increased its catalytic performance comparable to a reference platinum counter electrode.

Relevant to scaling up DSC preparation, a two way electrolyte filling method was studied as a means to suppress performance losses that occur due to non-homogenous distribution of electrolyte components. The method enhanced the photovoltaic performance of a segmented measurement cell by up to 42% compared to traditional one way filling of the electrolyte.

The aforementioned results provide pathways for the future development of robust flexible counter electrodes that can be beneficial especially from the perspective of high throughput roll-to-roll processing of flexible DSCs on polymer substrates.

Keywords Dye-sensitized solar cell, flexible substrate, ITO-PET, ITO-PEN, counter electrode, carbon composite, carbon nanotubes

ISBN (printed) 978-952-60-5625-8 **ISBN (pdf)** 978-952-60-5626-5

ISSN-L 1799-4934 **ISSN (printed)** 1799-4934 **ISSN (pdf)** 1799-4942

Location of publisher Helsinki **Location of printing** Helsinki **Year** 2014

Pages 52 **urn** http://urn.fi/URN:ISBN:978-952-60-5626-5

Preface

This work was completed during January 2010 to December 2013 in the New Energy Technologies (NEW) group, Applied Physics Department of Aalto University School of Science, Espoo, Finland and was financed through a project 'National Consortium for Low Cost Photovoltaic' by the Academy of Finland. I am thankful to Tekniikan edistämissäätiö (Finnish Foundation for Technology Promotion - TES) and Fortum Foundation for the travel grants to present my research work in the 28th European Photovoltaic Solar Energy Conference and Exhibition 2013.

I pay my special thanks to Almighty Allah for giving me the strength to accomplish this work and making it a reality as it was only a dream for me few years back.

I am very grateful to my supervisor, Professor Peter Lund, for selecting me to work on this extremely interesting research topic which offers plenty of challenges and opportunities to solve the key issues of this emerging technology as well as to furnish my capabilities by providing me an excellent research environment and facilities. I also thank my instructors Dr Janne Halme and Dr Kati Miettunen for their guidance, help and support to complete this research work.

I am so thankful to my parents, my wife Erum, my son Aarib, my brothers and rest of my family members for their prayers and support for my success in every stage of my life. I also thank my colleagues Dr Minna Toivola, Dr Mikko Mikkola, Dr Ying Ma, Dr Imran Asghar, Dr Albert Nasibulin, Dr Antti Nykanen, Dr Ilya Anoshkin, Dr Kerttu Aitola, Dr Simone Mastroianni, Dr Eeva Leena Rautama, Mr Tapio Saukkonen, Mr Henri Vahlman, Mr Antti Ruuskanen, Mr Erno Kemppainen, Ms Maryam Borghei, Mr Janne Patakangas, Mr Yifu Jing, Ms Armi Tiihonen, Mr Rami Niemi, Mr Jyri Salpakari, Mr Sami Vasala, for the fruitful discussions, help and advices throughout this period.

I pay special gratitude to late Z. A. Nizami, one of the founders and ex-chancellor of Sir Syed University of Engineering and Technology and to the ex-governor of Sindh, Shaheed Hakeem Mohammad Saeed and pray that Allah rewards both of them one of the highest place in Heaven for doing the great job for the students of Karachi city (Pakistan).

During my last year of PhD, I also visited Laboratory of Photonics and Interfaces (LPI) at EPFL University, Lausanne, Switzerland where I worked under the kind supervision of Professor Micheal Gratzel, Dr Sheikh Mohammad Zakeeruddin, Dr Thomas Moehl and other senior researchers. I thank all these people for their guidance and help during my stay at EPFL University.

Espoo, April 8th 2013

Syed Ghufran Hashmi

Contents

List of Publications

This thesis is comprised of the summary of following publications

I **Ghufran Hashmi**, Kati Miettunen, Timo Peltola, Janne Halme, Imran Asghar, Kerttu Aitola, Minna Toivola, Peter Lund, **Review of materials and manufacturing options for large area flexible dye solar cells**, Renewable and Sustainable Energy Reviews 15 (2011) 3717– 3732. http://dx.doi.org/10.1016/j.rser.2011.06.004

II **Ghufran Hashmi**, Kati Miettunen, Janne Halme, Imran Asghar, Henri Vahlman, Tapio Saukkonen, Zhu Huaijin, Peter Lund, **Comparison of plastic based counter electrodes for dye sensitized solar cells,** Journal of the Electrochemical Society, 159 (7) H656-H661 (2012). http://dx.doi.org/10.1149/2.059207jes

III Kati Miettunen, Minna Toivola, **Ghufran Hashmi,** Jyri Salpakari**,** Imran Asghar, Peter Lund, **A carbon gel catalysts layer for the roll to roll production of dye solar cells**, Carbon, 49, 528-532, (2011). http://dx.doi.org/10.1016/j.carbon.2010.09.052

IV **Syed Ghufran Hashmi**, Janne Halme, Tapio Saukkonen, Eeva-Leena Rautama, Peter Lund, **High performance low temperature carbon composite catalysts for flexible dye sensitized solar cells,** Physical Chemistry Chemical Physics, 15, (2013) 17689-17695, http://dx.doi.org/10.1039/C3CP52982G

V **Syed Ghufran Hashmi**, Janne Halme, Tapio Saukkanen, Peter Lund, **A Single-Walled Carbon Nanotube Coated Flexible PVC Counter Electrode for Dye-Sensitized Solar Cells** (Accepted for publication in Advanced Materials Interfaces). DOI: 10.1002/admi.201300055

VI **Syed Ghufran Hashmi**, Kati Miettunen, Antti Ruuskanen, Imran Asghar, Janne Halme and Peter Lund, **Process steps towards a flexible dye solar cell module,** Proceedings of the 27th European Photovoltaic Solar Energy Conference 27, pp. 2922-2924 (2012). http://dx.doi.org/10.4229/27thEUPVSEC2012-3DV.4.42

Author's contributions

The Doctoral Thesis was performed in the Department of Applied Physics, New Energy Technologies Group at Aalto University. The Thesis comprises of 6 publications. The author's contribution in these were the following:

Publication 1: The author was the main planner of this review article. He carried out immense literature survey and wrote all the major parts for this publication.

Publication 2: The author contributed in the designing, planning and analysis of the measured data. He also conducted all the photovoltaic and electrochemical measurements and wrote all the major parts of for this publication.

Publication 3: The author was actively involved in planning, designing and execution of the experiment. He prepared the carbon composite for the study and also contributed in fabrication of the devices. He was actively involved in measurements and data analysis for the publication and contributed to the writing.

Publication 4: The author designed the experiment and performed all the characterization of the experiment except for the SEM imaging. The author also designed and performed all the mechanical stability test for each carbon composites used in this work. He actively participated in the analysis of the results and wrote all the major parts of the manuscript.

Publication 5: The author is the main planner of the experiment. He developed the low temperature SWCNT ink for the PVC substrate. He conducted all the measurements except the SEM imaging and was actively involved in the analysis of the experimental study. He wrote all the major parts of the publication.

Publication 6: The author was actively involved in the planning, designing and execution of the experiments. He measured all the photovoltaic parameters and actively participated in the data analysis. He wrote all the major parts of the publication.

Abbreviations

CE	Counter electrodes
CNT	Carbon nanotubes
DSC	Dye sensitized solar cell
EIS	Electrochemical impedance spectroscopy
FTO	Fluorine doped tin oxide
HOMO	Highest occupied molecular orbital
ITO	Indium doped tin oxide
LUMO	Lowest unoccupied molecular orbital
MPP	Maximum power point
PV	Photovoltaics
PE	Photo electrode
PET	Polyethylene-terephthalate
PVC	Poly vinyl chloride
R2R	Roll-to-roll
SWCNT	Single walled carbon nanotubes
TCO	Transparent conducting oxide
TPCE	Thermally platinized counter electrode

Symbols

FF	Fill factor
GW	Giga watt
J_{SC}	Short circuit current density
η	efficiency
Pt	Platinum
R_{CT}	Charge transfer resistance
R_D	Diffusion resistance
R_{REC}	Recombination resistance
R_S	Series resistance
R_{SH}	Sheet resistance
Si	Silicon
Ti	Titanium
TiO_2	Titanium dioxide
V_{OC}	Open circuit voltage

1. Introduction

The modern life style is based on ample use of energy which is obtained mainly through the fossil fuels. These fossil fuels reserves are expected to provide 80% of the world energy demand by 2040 [1]. However, the adverse environmental effects from these traditional energy sources, notably the carbon emissions which contribute to the climate change, calls up to investigate alternative clean energy that could fulfill the energy needs of the mankind. This type of clean and abundant energy can be potentially obtained by utilizing photovoltaics (PV) technology at large scale. The solar resource is immense exceeding the global energy demand by a factor of several thousands. Photovoltaics technology (PV), which converts the sunlight to electricity without any moving parts, is a highly promising approach to harness the solar energy resource. In 2012, 31 *GW* of PV installations were reported worldwide which could be approaching nearly to 84 *GW* per year by 2017 [2]. The PV module cost has rapidly decreased during the last five years and the projected prices are expected to decrease further [3]. Ensuring future cutbacks in the PV prices will necessitate the development of cost efficient materials and technology in upcoming years. The Silicon (Si) based PV systems including 1st and 2nd generation solar cells have a 90% market share of all PV and [4]. Though the prices of Si based PV systems have dropped during the last years, to reach a level typical for a common commodity will require less expensive fabrication processes [4].

Nevertheless, the third generation organic solar cells and more specifically the dye sensitized solar cell technology (DSC) offers a possibility to lower the overall manufacturing cost due to their unique design, structure and having abundantly available cost efficient materials. Although the traditional geometry was engineered on transparent conducting glass, however, the same fabrication model can be transferred to flexible inexpensive polymer or metallic sheets [5]. This is an advantage over the Si solar cell in terms of variety of applications perceived. However, this transfer of technology from rigid glass substrates to flexible substrates requires solutions of key challenges associated with flexible substrates based DSC. For instance, the traditional glass based DSC utilizes such materials that can be deposited through a well-established screen printing process and followed by the high temperature sintering which is a key requirement

to remove the unwanted binders (that are added during the materials synthesis to make it in the form of a paste) as well as to improve the surface adhesion with the substrate. Despite of the rigidity of the glass substrate, it can handle higher temperatures (around 800 °C) without affecting its transparency.

The usage of PET polymer substrates restricts the temperature to 150 ºC as the polymer sheets starts to deform after that. Hence the post-sintering process on these low temperature polymer sheets cannot be applied. Therefore one of the key challenges is to develop low temperature based highly efficient materials that could give similar performance like deposited on glass.

1.1 Objectives of this study

The main motivation of this thesis was to find alternative material approaches to DSC with a potential for lower costs and higher module flexibility. The main focus of this study was therefore on different low cost alternative catalyst layers such as PEDOT-TsO or carbon composites on polymer substrates. The aim was to study the characteristics and their viability of low cost catalysts in the dye sensitized solar cell. Also, efforts were made to replace the expensive and scarce indium doped tin oxide (ITO) layer used in DSC with single walled carbon nano-tubes.

1.2 Outline of this thesis

The thesis work started with gathering information and knowledge on material and manufacturing options for flexible DSC cells, which was reported in the form of an extensive literature review as a review article (Publication 1). After that, systematic studies on low temperature catalyst layers were performed by implementing commercially available and in-house made low temperature inks and pastes of these catalysts (Publications 2-6).

The thesis consists of 5 individual chapters. Chapter 1 outlines the justification, scope, aims and contents of the thesis. Chapter 2 discusses the basic principles of operation of a dye sensitized solar cell. Additionally the Chapter 3 explains the cell fabrication, measurement procedures and characterization techniques used during the experimental studies in this Thesis. The results from all the experiments are discussed in Chapter 4. Finally, the key findings along with the idea of future work are concluded in Chapter 5.

2. Basics of dye sensitized solar cells (DSC)

2.1 Operating principle and device structure

Dye sensitized solar cells often called dye solar cell (DSC) is a photovoltaic device which consists of a photoelectrode (PE), a counter electrode (CE) and an electrolyte solution (Figure 1). The photoelectrode is comprised of a thick layer (10-20 μm) of semiconducting oxide (normally TiO_2) which is coated with a monolayer of light absorbing material (typically an organo metallic ruthenium sensitizer called 'dye') through sensitization of dye molecules. The dye molecule excites from highest occupied molecule orbital (HOMO) to lowest unoccupied molecule orbital (LUMO) upon receiving solar radiations (photons) and injects an electron into the conduction band of TiO_2 where it percolates/diffuses into the thick nanostructured TiO_2 medium and fetches by the external circuit through transparent conducting oxide (TCO) layer.

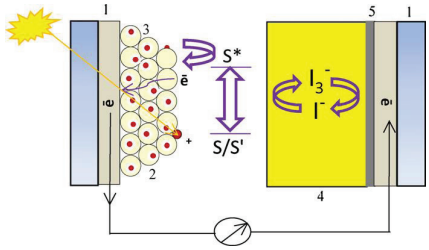

Figure 1. Structure of the dye solar cell: (1) conducting substrates, (2) TiO_2, (3) dye monolayer, (4) electrolyte, and (5) catalyst layer. (Reprinted from Publication 1with permission from Elsevier).

The iodide/tri-iodide (I^-/I_3^-) redox based liquid electrolyte solution regenerates/reduces the dye molecule by transferring an electron to the excited dye through the iodide ion (I^-) which oxidizes to tri-iodide ion (I_3^-) *and moves* towards the counter electrode. This oxidized I_3^- ion reduces back to I^- ion by receiving the electron from external circuit through a catalyst layer, typically platinum (Pt) and completes the process. The details of the overall electrochemical reactions is as follows

$$S + h\upsilon \longrightarrow S^* \text{ (Photo excitation)} \quad (1)$$

$$S^* \longrightarrow S^+ + e^- \text{ (TiO_2 injection)} \quad (2)$$

$$2S^+ + 3I^- \longrightarrow 2S + I_3^- \text{ (Dye regeneration)} \quad (3)$$

$$S^+ + e^- \longrightarrow S \text{ (Recombination)} \quad (4)$$

$$I_3^- + 2e^- \longrightarrow 3I^- \text{ (Reaction at the CE)} \quad (5)$$

Figure 2 illustrates the typical energy diagram of a DSC in which the difference between the Fermi level of semiconducting oxide (TiO_2) and redox potential determines the cell voltage whereas maximum absorption wavelength for photo-excitation is defined by the energy gap of HOMO and LUMO level of the dye (sensitizer) molecule.

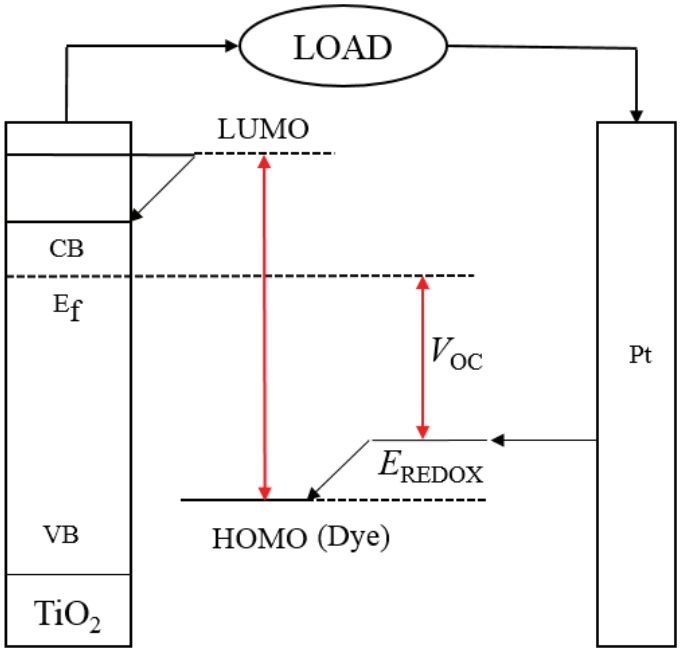

Figure 2. Energy level diagram of DSC.

Traditional fabrication and geometry of DSC was designed on rigid glass substrates loaded with a TCO layer. The highest efficiencies till date are recorded with glass based DSC both on lab sized (12.3%) [6] as well as on the module level (9.9%) [7]. The use of glass offers plenty of advantages, for instance, resistance against penetration of moisture and oxygen. Moreover, the glass based embodiments can also be integrated in building facades [8] and roof tops [8] due to these characteristics. Nevertheless, the glass sheet substrates have been realized as the most expensive among the cell components [9]. Also, glass sheets cannot be chosen for high volume roll-to-roll (R2R) production. Fortunately, it is possible to adopt modern printed electronics technology for fabrication of DSC by using light weight and flexible sheets of polymers and metals [10]. Metallic sheets have an edge over plastics in many distinguished features such as low cost, high con-

ductivity and moisture resistance in comparison with polymer sheets. Additionally metallic sheets are compatible with high temperature sintering processes which are the key requirements to get high quality and adhesive films of the desired materials. The highest efficiency (8.6%) till date for flexible DSC was reported in reverse illumination manner with an opaque metal PE and semitransparent chemically platinized CE [5]. However, one of the major issue related to these metallic sheets is the corrosion in the iodide/triiodide (I^-/I_3^-) redox medium present in the liquid electrolyte of the cell [11].

On the other hand, a critical challenge for plastic substrates is to produce durable films of the desired materials at lower temperature since the maximum temperature these plastics can endure is around 150 °C. Despite of the initial performances, the mechanical stabilities of low temperature based inks and pastes are rarely reported in the literature [12-14]. Without ensuring good adhesion on polymer substrates, the fabrication of robust DSC cannot be realized. These vital issues are key hurdles for the industrial production of DSC and require careful optimizations of not only the materials but also the processes that should be simple and rapid. Furthermore, the long-term operation of the flexible DSC is still questionable. There are very few reports that indicate the long term stability of flexible DSCs [15, 16].

3. Measurement procedures and methods

In the following, the central measurement and characterization methods used in this thesis are presented.

3.1 Photovoltaic parameters and IV measurements

IV measurements constitute the basic solar cell characterization method, important to determine the key performance parameters. The short circuit current density (J_{SC}), open circuit voltage (V_{OC}), fill factor (*FF*) and the cell efficiency (η) are the fundamental characterization parameters which can be obtained through current–voltage (*IV*) curve of the solar cell (Figure 3). The IV curves are normally recorded with a solar simulator in an artificial light intensity of 1000 W/m^2 which is equivalent to 1 Sun light intensity. The overall cell efficiency of the cell can be expressed by the following formula:

$$\eta = \frac{P_{max}}{P_{in}} = \frac{J_{SC}.V_{OC}.FF}{P_{in}} \qquad (6)$$

Where P_{max} is the product of I_{MPP} and V_{MPP}. The I_{MPP} and V_{MPP} are the maximum current and voltage that can be drawn at maximum power point (MPP) of the cell as shown in Figure 3. Additionally the FF can be expressed as

$$FF = \frac{V_{MPP}.I_{MPP}}{V_{OC}.J_{SC}} \qquad (7)$$

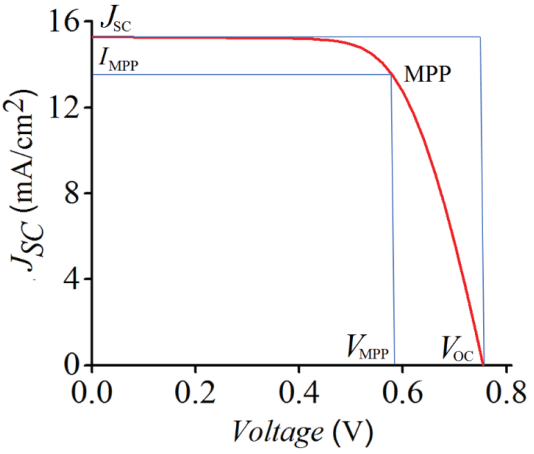

Figure 3. Typical IV curve of DSC.

3.2 Electrochemical impedance spectroscopy

The electrochemical impedance spectroscopy is an established tool for DSC that is used to measure impedances of the individual cell constituent and their interfaces with other components of the cell. The motivation of using this technique is the estimate of losses at different current and voltage values which cannot be identified through simple *IV* curve. These interfaces build *RC* circuits which exhibit different impedance responses due to the different time constants. The electrical modelling (Fig. 4) of the physical device (DSC) allows the fitting of the response of these physical components and interfaces which results upon the scanning of a range of frequencies (typically from 100 mHz to 100 kHz).

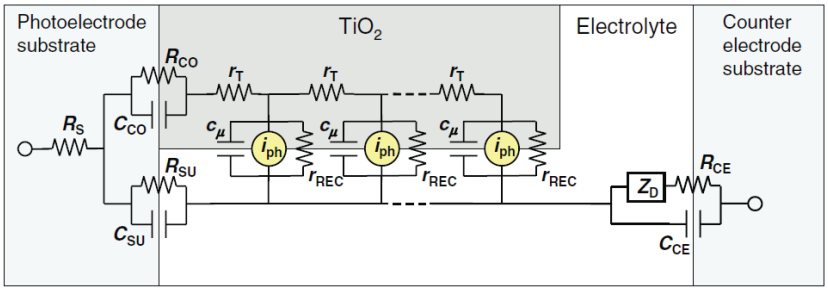

Figure 4. Electrical model of physical device (DSC) Copyright Wiley-VCH Verlag GmbH & Co. KGaA. Reproduced from reference [17] with permission.

The fundamental parameters of the models (Fig. 4) are defined as follows:

r_T = Resistivity of electron transport in the photo electrode film, consisting typically of interconnected TiO_2 nanoparticles. The total transport resistance of the film is $R_T = r_T d$ where d is the film thickness.

r_{REC} = Charge transfer (recombination) resistance at theTiO_2/dye/electrolyte interface per unit volume of the electrode. The total recombination resistance of the film is $R_{REC} = r_{REC} d^{-1}$.

R_S = Ohmic series resistance of the cell. The total R_S is the sum of contributions from the sheet resistance of the substrates, resistivity of the electrolyte and electrical contacts and wiring of the cell.

R_{CE} and C_{CE} = Charge transfer resistance and double layer capacitance at the counter electrode electrolyte interface.

Z_D = Mass transport impedance at the counter electrode.

R_{CO} and C_{CO} = Contact resistance and capacitance at the interface between the conducting substrate and the TiO_2 photo electrode film.

R_{SU} and C_{SU} = Charge transfer resistance and double layer capacitance at the substrate/electrolyte interface.

Among the above mentioned circuit parameters, Rs, R_{CO}, r_T, Z_D, and R_{CE} directly affect the *FF* in the *IV* curve of DSC and consequently the efficiency. Additionally the R_{REC} affects the open circuit voltage (V_{OC}) whereas the R_{SU} should be high enough to block the current leakage from photo electrode to the electrolyte.

The electrochemical impedance response can be represented through so-called Nyquist plots and their corresponding frequency peak positions can be identified through imaginary impedance (*-Z''*) vs frequency plot as shown in Figure 5 a-b respectively.

In the Nyquist plot, the distance from the origin to the first semicircle represents the series resistance (R_S) whereas the first semicircle corresponds to the charge transfer resistance (mostly denoted by R_{CT}) at the counter electrode/electrolyte interface. The second semicircle in the Nyquist plot represents the resistance of photoelectrode or 'recombination resistance (R_{PE})'. The third very small semicircle of the complete response represents the electrolyte diffusion resistance (R_D). The typical values for R_S mainly depends upon the sheet resistance (R_{SH}) and for DSC, it ranges from 5 Ω/Square to 60 Ω/Sq [18]. On the other hand the good R_{CT} values are considered to be less than 10 Ωcm^2.

Moreover, the traditional thermally platinized counter electrode (TPCE) based DSC exhibits three frequency peaks in the frequency range between 100 mHz to 100 kHz. The first semicircle for TPCE is associated with the charge transfer resistance (R_{CT}) which appears in very high frequency (> 1 kHz) range [19]. Additionally the second adjacent semicircle corresponds to the recombination resistance of the photo electrode (R_{PE}) and its characteristic frequency appeared around 20-30 Hz [19]. The third small semicircle that appeared at very low frequency (~ 1 Hz) is associated with the diffusion resistance (R_D) of the cell [19].

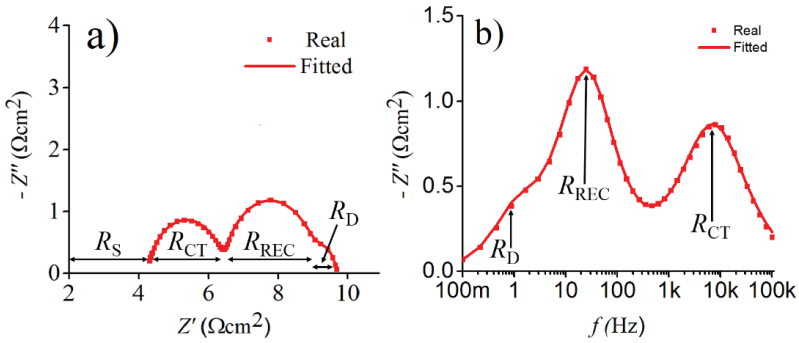

Figure 5. Typical EIS response of the DSCs measured at V_{OC} under illumination represented as a) Nyquist plot, b) imaginary impedance Z'' as a function of frequency *f*. All solid lines correspond to the fitted data whereas the points represent the measured (real) data.

3.3 Incident photon-to-collected electron efficiency (IPCE)

The incident photon-to-collected electron efficiency (IPCE) is a measure of the current production as a function of the wavelength. This technique is used to observe the spectral response of the solar cell which describes how many electrons the external circuit receives against the number of photons having a certain wavelength (λ). The partial quantum efficiencies, i.e. light harvesting (η_{LH}), electron injection (η_{INJ}), charge collection (η_{COL}) and regeneration (η_{REG}) efficiency, define the total incident photon to collected electron efficiency (η_{IPCE}) as

$$\eta_{IPCE}(\lambda) = J_{SC}(\lambda)/q\varphi(\lambda) = \eta_{LH}(\lambda).\eta_{INJ}(\lambda).\eta_{COL}(\lambda).\eta_{REG}(\lambda) \qquad (8)$$

in which $\varphi(\lambda)$ is the photon flux at a given wavelength λ and q is the elementary charge. Figure 6 represents typical IPCE data of the cell when illuminated from the PE side of the cell. The charge collection losses can be determined from the CE side illumination of the cell that cause a so-called 'red shift' in the peak IPCE spectrum.

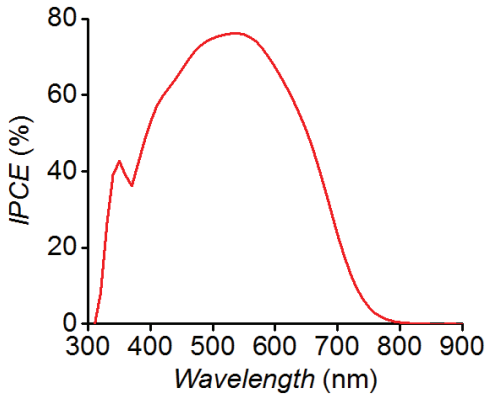

Figure 6. Typical IPCE spectrum of DSC.

3.4 Mechanical adhesion tests

One of the key challenges in case of formulation of low temperature pastes is the adhesion of deposited materials since they do not experience the high temperature sintering step which is critical in case of glass or metal substrates. The high temperature sintering step does not only promote the interparticle connection within the material but it also gives strong adhesion with the surface of the substrate. These adhesive and mechanical properties significantly affect the overall performance of the device (DSC). However, the case for plastics is different where the temperature restriction remains under 150 °C. It is therefore very important to check the mechanical strength of low temperature inks over the substrates. We adopted two recognized mechanical test procedures for Publication 3 and 4 for the determination of mechanical stability of the material. The first one is called bending test while the other one is called tape adhesion test [20]. For Publication 3, only qualitative analysis of mechanical stability was made whereas it was demonstrated in more detail for Publication 4. For Publication 4, the deposited carbon nanotube (CNT) ink was bended over different bending radius and the resistance (R) was regularly measured. The value of resistance was then used to measure the sheet resistance (R_{SH}) of the CNT loaded substrate with the help of following formula i.e.

$$R_{SH} = (R^*W)/L \qquad (9)$$

Where W and L are the width and length of the film respectively between the electrical contacts. Moreover, the same resistance was measured in case of a tape

test where the deposited CNT film was rolled with a heavy roller under the pressure sensitive test and the tape was pulled at 90° angle and the resistance was regularly measured.

3.5 Scanning electron microscopy

The surface morphologies of the deposited layers in the publications were recorded with JEOL JSM-7500FA and Zeiss Ultra 55 FEG-SEM Scanning electron microscopes. Additionally in Publication 4, the Bruker AXS energy dispersive analyzer (EDS) was also used to identify different particles of the carbon composites.

3.6 Cell fabrication

In each experimental study, the photo electrodes were prepared on FTO glass (TEC-15, Sheet Resistance = 15 Ω/Sq, Pilkington) by utilizing screen printing of commercially available TiO_2 pastes (Dyesol). The reference Pt counter electrodes (CE) were prepared on FTO glass (TEC 15, Sheet Resistance = 15 Ω/Sq, Pilkington) by thermal platinization of 5mM solution $H_2Pt_6Cl_4$ precursor in 2-Propanol. The details of unique low temperature catalyst layers are mentioned in the included publicatons. In short, the conducting polymer (PEDOT-TsO) catalyst layers were deposited both on ITO-PET (Publication 2) and on SWCNT coated PVC substrate (Publication 5) by spin coating whereas the low temperature Pt catalyst layers (Publications 2 and 6) were deposited on ITO-PET and ITO-PEN polymer sheets by chemical platinization and electrochemical platinization methods described in the relevant publications. The sandwich type cell assemblies were fabricated by separating the PE and CE with either Surlyn or Bynel frame foils which also determines the cell channel. High stability electrolyte coded as HSE (which contains 1-propyl-3-methylimidazoliumiodide (PMII), iodine (I_2), guanidinumthiocyanate and benzimidazole) from Dyesol was injected in most of the studies. Then the cells were sealed with the Surlyn or Bynel polymer and a thin glass cover with a hot press. The contacts of the solar cells were fabricated with a copper tape and quickly drying silver ink.

4. Results and discussions

The experimental study is comprised of 6 individual publications and the main area of research was low temperature catalyst layers as alternative counter electrodes for DSC. The motivation was to find out the possibilities/ways to replace some expensive components of the DSC for instance expensive FTO Glass with cheap polymers, Pt catalyst layer or expensive and scarce ITO layer with alternative materials.

4.1 Fabrication options of dye sensitized solar cells on flexible substrates (Publication 1)

The thesis research was started with a review article about the state of the art regarding the commercialization and up-scaling options of dye sensitized solar cells fabricated mainly on alternative (flexible substrates). Also the aim was to present a general cost analysis about the materials that are presently available for this technology and the realization of an ideal fabrication step model of dye sensitized solar cell for continuous roll-to-roll processing.

4.1.1 Cost overview for dye sensitized solar cells

The cost of volume production of dye solar cells technology mainly depends on the materials cost and the fabrication techniques. For DSC, there are plenty of options for inexpensive materials, for instance, titanium dioxide (TiO_2) or carbon (C) with abundant availability to be tested along with quick and easy fabrication methods which cannot only lower the cost but can also potentially speed up the manufacturing processes. Also, the conventional expensive and rigid glass substrates which have been used for batch processes can be replaced with cheap and flexible substrates such as inexpensive polymers, metals or even paper [21]. Moreover, the usage of flexible substrates can extend the integration of DSCs in various applications such as in clothes, school bags and other commercial products. Nevertheless the main challenge for these low cost substrates is the low temperature fabrication processing of the materials on them along with high durability and strong mechanical stability. Long-term and stable operation of fully flexible DSC is vital for the competitiveness against the conventional Silicon based solar cells which is offering 20 years of warranty at present.

The rigid glass substrate is the most expensive component in a DSC: its share is around 80% of the cost among all the active components of the cell such as TiO_2 nanoparticles, platinum (Pt) or carbon catalyst materials, dye or electrolyte [9]. The overall cost can be significantly decreased (35%) if these expensive substrates could be replaced with polymer substrates [9]. Additional reduction in the cost (99%) is possible if the polymers could be replaced with commonly available aluminum (Al) foil (Table 1).

Table 1: Approximated costs of different materials of DSC. The costs presented for substrates are based upon single substrate cost. (Reprinted from Publication 1with permission from Elsevier).

Components	Cost ($/m^2)	References
<u>Single substrate</u>		
1) TCO Glass	12.5-25	[9]
2) ITO-PET	8 – 72 [a]	[9, 22]
3) Titanium (Ti) mesh	15-20	[23]
4) Ti foil	90	[24]
5) Stainless steel (StS)	4	[25]
6) Aluminum (Al) foil	0.055	[26]
<u>Other active materials</u>		
TiO_2 particles	0.04	[9]
TiO_2 paste	29	[27]
Electrical connections	2.9	[9]
(Dye, electrolyte, catalyst)	10.3	[9]
<u>Inactive materials</u>		
Sealants, laminating Materials, encapsulants, Additional wiring for external connections and laminating materials.	29	[27, 9]

The need to make the pastes or inks from raw materials by utilizing low cost synthesis techniques is also vital as the cost of screen printable TiO_2 paste was estimated 1000 times higher ($29/m^2) than the cost of TiO_2 nanoparticles ($0.04/m^2) (Table 1). Another advantage of flexible DSCs is avoiding the cost for inactive materials such as metallic frames, strut and bolds and additional glass encapsulations used in the installations of silicon solar cells. Zweibel reported $5/m^2 for these inactive components [25]. The potential for further cost reductions is also possible by replacing other costly materials such as Pt [28] or ITO [29] layer with much cheaper catalyst and conductive materials such as carbon nano-particles [30].

Another favorable aspect for the DSC is the cost of its manufacturing tools and equipment. For a 10 MW/year manufacturing capacity, the production costs for glass based DSC has been estimated in between \$7.25/m^2 - \$11.60/m^2 [9] compared to \$32/m^2 production cost for thin film solar cells [25]. Hence by fabricating DSCs on light weight flexible substrates and implementing roll-to-roll processing, large cost reductions could be expected and could even be halved compared to glass-based batch process DSC technology. Presently, silicon photovoltaic modules are sold at a cost less than \$1/W_P which has been achieved through scale of economics and increasing competition. In case of DSC, which is still in a laboratory phase, scaling up to mass production should most likely bring down the cost further through different learning and scale effects in production. The easy and non-vacuum based fabrication equipment for DSC may potentially further reduce the overall cost down to \$ 0.4/W_P in production cost with 100 MW yearly production capacity [31].

4.1.2 Realization of flexible dye solar cells

As mentioned earlier, the DSC fabrication process can be switched from traditional glass substrates to either flexible polymer or metallic sheets and can be fabricated in different combinations as shown in Figure 7 a-c. There are key challenges associated with each type of configuration. For example, the whole cell assembly can be fabricated on transparent conducting oxide coated flexible polymer sheet (Figure 7 a) like the typical glass based DSC if the materials could be deposited or coated using low temperature pastes and inks. On the other hand, the metals can be configured either as PE [5] or CE [32] (Figure 7 b-c). However, the optics in case of utilizing metals as a PE requires careful optimizations to achieve maximum output power since the cell is illuminated from the CE side and the light is absorbed by the TCO, the semi-transparent catalyst layer as well as the electrolyte. In case of a metal as a CE will require a high performance low temperature TiO_2 ink/paste coated PE on TCO plastic [33] which is a crucial challenge in the realization of flexible DSCs.

Long term stability is vital for the success of flexible dye solar cells. These cells need to stand high humidity and extreme temperatures. The UV sensitivity of plastics can also be a severe problem for flexible DSC compared with glass [34].

In this regard the integration of flexible DSC needs to be reviewed according to its application in different operating conditions. The good news about the DSC is its higher relative performance in low light conditions compared to Silicon based solar cells [35]. This can broaden the utilization of flexible DSC e.g. for battery charging of mobile phones, school bags and clothes where both bright light and extreme weather conditions are not necessarily required for the optimum operation of DSC. Some low light working demonstration of DSC has already been shown from G24i [10] and Sony [36].

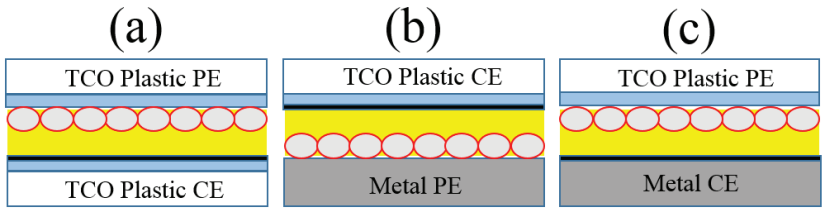

Figure 7. Different configurations of flexible dye sensitized solar cells. TCO = Transparent conducting oxide, PE = Photoelectrode, CE = Counter electrode.

4.1.3 Flexible photo electrodes

Flexible photoelectrodes can be fabricated by utilizing fast roll-to-roll fabrication devices. The metal based photoelectrode offers an advantage for high temperature sintering processes which is a key requirement for a high quality TiO_2 nano particles film. These high temperature TiO_2 nanoparticle films have been employed in the reverse illumination type DSC [5] (as discussed in section 4.1.2) and has achieved an efficiency of 8.6% [5]. On the other hand, the high temperature sintering process cannot be applied on plastic substrates such as ITO-PET or ITO-PEN because they start to deform after 150 °C. Transferring the high temperature TiO_2 sintered film has been demonstrated through a so-called 'lift off' process [37]. The key issue related to low temperature inks is the weak inter-particle bonding between individual TiO_2 particles which is typically obtained through the high temperature (~ 500 °C) sintering process. Hence the movement of electrons within the film experiences high resistance and causes lower currents compared to high temperature TiO_2 film. Several groups demonstrated different low temperature methods such as chemical sintering [38], TiO_2 film pressing [33, 39] and ball milling [38, 39], hydrothermal treatments [40], as well as different UV, microwave or laser sintering methods [41, 42]. Utilizing aforementioned methods, efficiency levels of 6-8% has been obtained with plastic DSCs which is still

lower than the glass based DSCs. Table 2 summarizes the range of efficiencies obtained through different techniques.

Table 2: List of efficiencies obtained by implementing flexible photo electrodes in DSC. (Reprinted from Publication 1with permission from Elsevier).

Substrate	Paste	Deposition	Post treatment	η (%)	Ref (Pub)
StS	TiO_2, Alpha-terpinol and ethyl cellulose	Doctor blading	Sintering 600 °C	8.6	5
ITO-PEN	TiO_2-water paste	Doctor blading	Mechanical pressing	8.1	33
Ti	TiO_2 paste	Screen printing	Sintering	7.2	43
ITO-PEN	(1) TiO_2 F-5 Showa titanium t-butanol and water (1:2), (2) aqueous collide TiO_2 (brookite) 21 wt.%, 25% HCL with pH4 and 75% ethanol, (3) mixture of (1) and (2)	Doctor blading or screen printing	Heating at 110 – 125 °C	5.8	44
Glass	Stock solution of Ti4+ Titanium(iv) isopropoxide, triethanolamine and DI	Thermal hydrolysis	Mechanical compression	5.8	40
ITO-PET	TiO_2 F-5 Showa titanium tert-butyl alcohol and acetonitrile (95:5) mixture	Electrophoretic deposition	CVD/UV 254 nm	3.8	41
ITO-PET	TiO_2 P25 Degussa, water, nitric acid, Triton, ethanol and methanol	Spray deposition or pulsed laser	UV 248 nm pulse width 20 ns	3.3	42
ITO-PET	TiO_2 P25 Degussa [Ti(IV)-tetraisopropoxide]	Hydrothermal crystallization	Autoclaving 100 ◦C 12 h	2.5	40
IT-PET	TiO_2 P25 Degussa, 20 wt.% ethanol	Doctor blading	Mechanical pressing	2.3	45

4.1.4 Flexible counter electrodes

Like the photoelectrodes, the characteristics of the counter electrodes, e.g. the charge transfer resistance (R_{CT}), reasonable transparency in case of reverse illumination as well as a good adhesion of the catalyst material affect the overall

performance of the DSC (mainly the *FF* of the *IV* curve). Different catalyst layers e.g. Platinum (Pt) [18], carbon composites [19], conducting polymers (i.e. PEDOT:PSS or PEDOT:TsO) [46] or carbon nanotubes [47] have been tested in different experiments. Among them the conventional Pt can be deposited through various available low temperature techniques such as chemical platinization [5], electrochemical platinization [18], or sputtering [48, 49]. The advantage in case of electrochemical platinization and sputtering is the realization of semitransparent layers that can be obtained through the optimization of deposited parameters and can be implemented in a reverse illuminated DSC. The cost will be an issue in these cases. Also semi-transparent carbon nanotubes as a catalyst substitute are deposited via a dry transfer process [47] but this did unexpectedly not exhibited good catalytic activities and requires an additional catalyst layer [47]. On the other hand, opaque films of carbon composites can be used by the conventional doctor blading method [19]. A problem with carbon materials as catalysts is the adhesion with the substrates and the mechanical stability of these which is rarely reported in the literature. Conducting polymers such as p-toulenesulfonate-doped poly (3, 4-ethylenedioxythiophene) (PEDOT-TsO) or polystyrenesulphonate (PSS) have also been tested as an alternative catalyst material via spin coating or screen printing on polymer foils [50, 51]. The best efficiency (7.93%) for these polymers is reported through electrochemical polymerization [52] among all reported methods such as spin coating or screen printing.

4.2 Stability issues of flexible DSCs

The DSCs manufactured on glass substrates have exhibited high efficiencies along with excellent stabilities under 60 °C and 80 °C accelerated aging tests and also in outdoor natural environmental conditions [53-56]. This is mainly due to the excellent resistance of glass against the moisture intrusion as well as the temperature. The case for flexible substrates such as polymer and metallic sheets is entirely different. The plastic sheets are permeable and thus allow the intrusion of water/moisture within the cell [15]. In this case the selection and suitability of materials that could resist the moisture is important. For example the traditional N719 is known to be hydrophilic which means it is capable of absorbing water [11]. The mechanical stability of the materials is also a key factor for the high performance. The scientific reports for low temperature inks and materials based DSC rarely state mechanical stability data or tests. The plastic substrates are also

sensitive to UV light as well as harsh volatile solvents such as acetonitrile. Flexible metallic sheets such as stainless steel are mainly affected by corrosion through the redox couple [11]. Currently the G24i is producing flexible DSC on Titanium (Ti) metal which is also considered as the expensive metal (i.e. \$ 90/m^2) [24].

4.3 Ideal process flow for the module production of flexible DSCs

We suggest an advanced *R2R* fabrication model for the flexible DSC by selecting all low temperature fabrication processes as shown in Figure 8. The best choice could be a plastic based photo electrode loaded with a binder free TiO_2 paste in order to minimize the optical losses. In addition to that, the method for dye staining is critical and requires more research to develop rapid staining techniques as it takes several hours to adsorb over the mesoporous layers of TiO_2 which is inappropriate to be integrated in the *R2R* manufacturing. Also the dye could be deposited either by inkjet printing or by screen printing. We consider the electrolyte injection in the cell channels and its composition as the most challenging part. Ideally a screen printable non-corrosive solid state electrolyte layer is recommended. The non-corrosiveness would be a key factor for using cheap metal substrates, e.g., Al or abundant Ag inks for preparation of fine metal grid over carbon nanotubes coated plastic substrate could omit protective layers and could reduce the inactive space.

Counter electrode materials can also be deposited either by low temperature inkjet printing or screen printing of either carbon composite or carbon nanotubes based inks. Usage of highly conductive carbon nanotubes can potentially reduce the overall cost due to removal of expensive ITO layer on the substrate if a plastic substrate is also used on the counter electrode. The complete module can then be assembled by applying adhesive on one of the electrodes and compressing both the flexible substrates together. Printable sealant material is recommended in process line via screen printing step followed by pressing [57]. Lastly, a barrier foil which is required to prevent moisture penetration could be laminated with an adhesive.

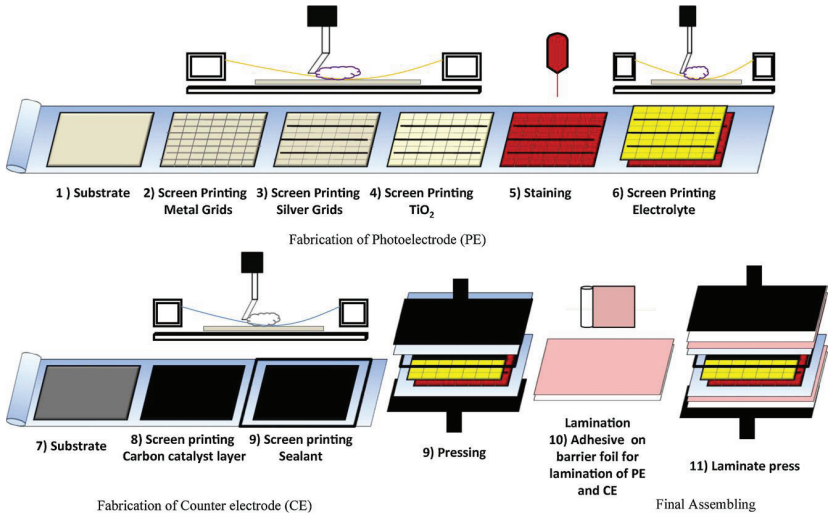

Figure 8. Process steps for the fabrication of flexible dye sensitized solar cells. (Reprinted from Publication 1with permission from Elsevier).

4.4 Characteristics of flexible counter electrodes

After the technology review, the main topic of research was alternative catalyst based counter electrodes where the characteristics/comparisons of several counter electrodes were studied in terms of photovoltaic performance, scanning electron microscopy (SEM) imaging, electrochemical impedance spectroscopy (EIS), incident photon-to-collected electron efficiency (IPCE). Moreover the studies on composites of carbon as an alternative catalyst layer and replacement of expensive ITO layer with carbon nanotubes was targeted due to their high conductivities and strong mechanical properties on polymers. The successful replacement of ITO is shown on a commonly available polyvinyl chloride (PVC) sheet with single walled carbon nanotubes.

4.4.1 Comparison of flexible counter electrodes (Publication 2)

During the literature review, several low temperature counter electrodes preparatory methods were identified but their performances being separately investigated in individual studies [19, 46]. Also the PE geometries in these individual studies were unique. Therefore, the counter electrodes cannot be compared with each other based upon their overall individual efficiencies. The main motivation was to identify the best polymer based counter electrodes for their utilization in both the direct and reverse illumination configuration for TCO coated flexible poly-

mer and metal photoelectrode respectively. The different low temperature semitransparent catalyst layers were obtained through chemical or electrochemical platinization and spin coating of PEDOT as well as a completely opaque carbon gel catalyst layer were also tested by keeping the same PE geometry. The optical characteristics along with the morphology and electrical performance were also investigated and compared with the reference glass based thermally platinized counter electrodes. The morphologies of the deposited layers are shown in Figure 9. From these images, the carbon based catalyst layers revealed highly porous structures thus offering high surface area in comparison with the platinized counter electrodes. On the other hand, a relatively non-uniform PEDOT layer (that was deposited via spin coating) was obtained over the ITO PET with certain uncovered areas which formed gaps ranging from 1 to 4 µm.

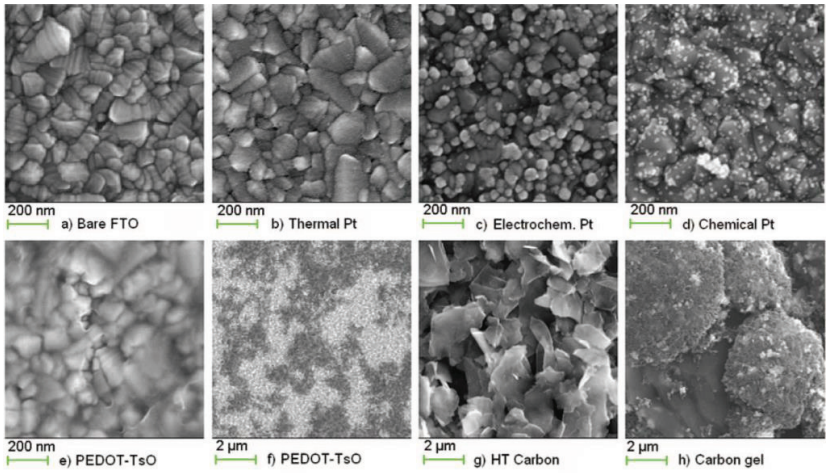

Figure 9. SEM image of a) Bare FTO Glass substrate and FTO glass substrate with b) thermal platinum, c) electrochemical Pt, d) chemical Pt, e) PEDOT-TsO (close up), f) PEDOT-TsO, g) HT carbon paste, and h) plastic carbon gel. (Reprinted from Publication 3 with permission of ECS).

The performance comparison showed the highest short circuit current densities (J_{SC} = 8 mA/cm^2) with chemical platinized counter electrodes values upon reverse illumination. The reason for the relatively higher J_{SC} values was explained with the optical properties of the counter electrodes e.g. the difference in the transmittances determined the differences in the in J_{SC} values for each type of counter electrode. The photocurrents in case of the opaque carbon catalyst layers with CE illumination are very small and such catalyst layer are practically suitable only for the PE side illumination. Additionally the same chemical platinized counter electrodes based DSC exhibited the highest efficiency with both the PE

(4.3%) and CE (3.1%) among all types. Surprisingly the PEDOT-TsO counter electrode based DSC exhibited 20% lower current densities which also affected its overall efficiency (3.3% from PE side and 2.2% from CE side).

The lower currents in the PEDOT counter electrode based DSC have already been reported in other studies [47]. For PEDOT base counter electrodes, it was initially assumed that some other factors such as electron injection, regeneration or collection efficiencies may limit the J_{SC}. Some of the above mentioned factors were investigated through incident photon-to-collected electron efficiency (IPCE) measurements which were conducted from both the PE and CE sides. It is well known that if there are collection losses, this directly produce the so-called 'red shift' of the peak position when IPCE is measured from the CE side. This peak shift was not found in all other types of cells, whereas for PEDOT the estimation of peak position was difficult. The difference between the PEDOT-TsO and the other cells was further investigated by calculating the IPCE ratio of the PEDOT-TsO and electrochemically platinized cell which revealed a significantly lower IPCE ratio (i.e. $\eta_{IPCE,CE}$ divided by $\eta_{IPCE,PE}$) for PEDOT-TsO cells compared with the electrochemical platinized counter electrode. Since each type of cell has the same photoelectrode, substrate and electrolyte composition, it is presumed that the PEDOT-TsO cells had lower η_{COL} or, in other words shorter electron diffusion lengths. One hypothesis for the reason for this could be that residues of PEDOT polymer had detached or dissolved in the electrolyte, diffused to the PE and adsorbed on the TiO_2 film, catalyzing the electron recombination reaction there.

The resistances for each type of counter electrode were determined with EIS measurements of the complete DSC. The carbon based electrodes exhibited lower series resistance (R_S) compared to other types of flexible counter electrodes whereas the highest catalytic activity, i.e. the lowest charge transfer resistance (R_{CT}), was recorded with PEDOT-TsO (2.8 Ωcm^2) and chemical platinized (3.7 Ωcm^2) counter electrodes which are comparable with the reference thermally platinized counter electrodes (2.6 Ωcm^2). Also, the low temperature carbon gelatinized catalyst layer had lower (~ 11 Ωcm^2) resistance than the high temperature carbon counter electrode on glass (17 Ωcm^2). It could be seen from the SEM images that the carbon gel catalyst layers exhibited larger surface area

compared to the high temperature carbon paste which was actually a film of graphite flakes. This caused the superior performance of carbon gelatinized catalyst layer compared to the high temperature carbon catalyst.

In conclusion we may say that a low temperature carbon gel catalyst layer can be a good option to be integrated with the best performing plastic photoelectrode, but its charge transfer resistance needs to be improved which may be potentially reduced by milling the composite that might increase not only the surface area but may also break down unwanted gel particles. On the other hand, the chemical platinized catalyst layer was found suitable in case of reverse illumination, but the cost can be an issue.

4.4.2 Characteristics of carbon composites catalysts in DSC (Publication 3 and 4)

The carbon composites offer an alternative solution to replace the expensive Pt catalyst layer in the DSC. Four different types of low temperature pastes of composites of carbon were formulated to test their viability in DSC. A systematic comparison was made in terms of mechanical stability, photovoltaic and electrochemical properties. In these experiments we first developed a carbon composite paste that was gelatinized with a polymer (polyvinylidenefluoride-co-hexafluoropropylene, PVDF-HFP). The flaking of low temperature carbon nanoparticles over plastic substrate is a well-known problem in DSC. Keeping that in mind the gel was added to the carbon composite for keeping the particles together as well as to promote the adhesion with the substrate (ITO-PEN).

In Publication 4, three different types of carbon composites namely binder free carbon composite (BFCC), TiO_2 nanoparticles as binder enriched carbon composite (BCC) and PEDOT polymer enriched carbon composite (PCC) were tested. The mechanical stability tests were done in a systematic way (see supporting information for Publication 4). First the bending tests with the carbon gel catalyst was performed which showed high elasticity of doctor bladed carbon layer and no flaking was seen. A higher charge transfer resistance (23 Ωcm^2) compared to the reference thermally platinized counter electrode (12 Ωcm^2) was obtained because of the gelator which cannot be removed due to the temperature

restriction of plastics (150 °C). This was taken as a compromise in between the elasticity and the catalytic activity.

Table 3: Adhesion characteristics of carbon composites deposited on FTO Glass, ITO-PEN and ITO-PET Sheets. (Reproduced from Publication 4 with permission from PCCP Owner Societies).

Substrate / Catalyst*	Dominant way of detachment of the film from the substrate		
	Particles from film	Parts of the film (10-30%)	Most of the film (> 90%)
FTO Glass-BFCC			X
FTO Glass-PCC	X		
FTO Glass-BCC		X	
ITO PEN-BFCC		X	
ITO PEN- PCC		X	
ITO PEN-BCC			X
ITO PET-BFCC		X	
ITO PET-PCC		X	
ITO PET-BCC	X		

*FTO=Fluorine doped tin oxide, ITO=Indium doped tin oxide, PEN= Polyethylenenaphtalate, PET=Polyethyleneterephtalate, CE=Counter electrode, PE=Photoelectrode, BCC=Binder carbon composite, PCC=PEDOT carbon composite, BFCC=Binder free carbon composite.

The bending and tape adhesion tests were also performed over the BFCC, BCC and PCC catalyst layers on three (FTO glass, ITO-PEN and ITO PET) substrates in Table 3. Among them the PEDOT enriched carbon catalyst layers exhibited better adhesion than the other two types over each substrate. The TiO_2 binder enriched carbon composite showed relatively good adhesion on ITO-PET, but on ITO-PEN its adhesion was poor.

In terms of photovoltaic performance, the carbon gel catalyst layer achieved an overall efficiency of 4.2% compared to 4.8% reference platinum counter based DSC (see Publication 3). The highest efficiency DSC engineered with BCC

reached 85% of the solar energy conversion efficiency (5.9%) of the reference DSC with platinum counter electrode (7%, see Publication 4).

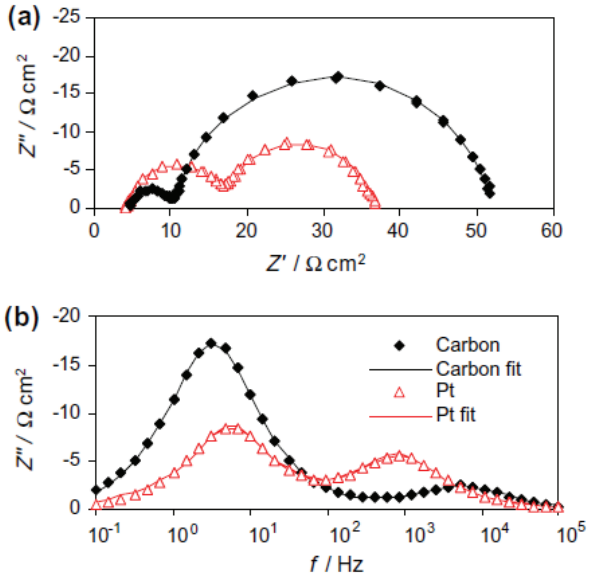

Figure 10. Typical EIS response of a complete DSC of reference thermally platinized counter electrode (red) and carbon composite based counter electrode (black). (Reprinted from Publication 3 with permission from Elsevier).

Figure 10 (a-b) represents typical EIS spectra of complete DSC fabricated with carbon composite counter electrodes on ITO-PEN (black) and the reference thermally platinized counter electrode (red). Figure 10a is the 'Nyquist plot' whereas Figure 10b is the imaginary impedance versus frequency range. All the EIS measurements reported in Publication 3 and 4 were performed in an artificial solar simulator under 1000 W/m^2 equivalent to 1 Sun light intensity and open circuit voltage conditions. The EIS frequency range was from 100 mHz to 100 kHz. The impedance arcs for each type of DSC can be identified in the Nyquist plot (Figure 10a and 11a) according to their unique peak positions shown in Figure 10b and 11b. For instance the reference thermally platinized counter electrode based DSC reveals three impedance arcs within 100 mHz to 100 kHz (Figure 11 a-b). The arc which appears at very high frequency range (> 1 kHz to 10 kHz) translates the charge transfer resistance (R_{CT}) at the counter electrode. On the other hand, two low frequency arcs which appear around 1-10 Hz and 20-30 Hz can be interpreted as the diffusion resistance (R_D) and resistance of photo electrode or 'recombination resistance' (R_{REC}) respectively (Figure 11 a-b).

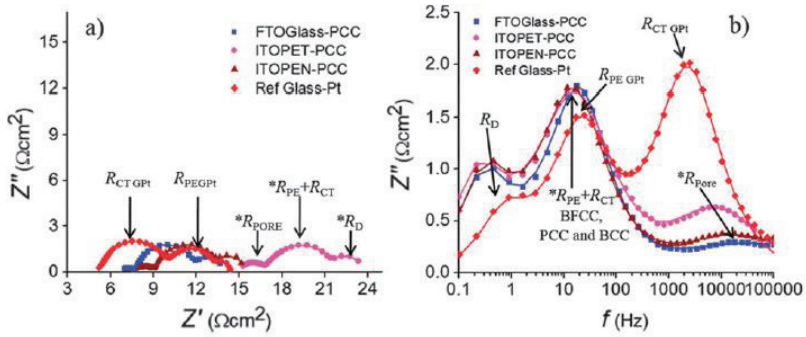

Figure 11. Typical EIS spectra of complete DSCs with PEDOT–carbon composite (PCC) catalyst layer counter electrodes on glass, ITO-PET, ITO-PEN and a reference thermally platinized counter electrode on glass. (a) Nyquist plots, (b) imaginary impedance Z'' vs. frequency. * These impedance positions are also valid for FTO glass PCC and ITO-PEN PCC. (Reproduced from publication 4 with permission from PCCP Owner Societies).

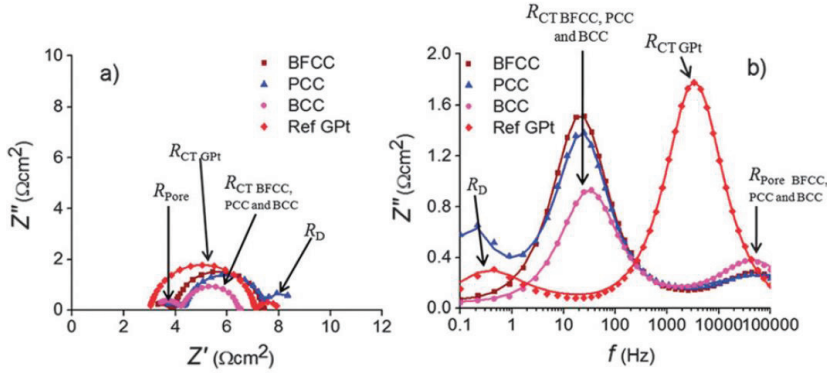

Figure 12. EIS spectra of CE–CE configurations (a) Nyquist plots, (b) imaginary impedance Z'' as a function of frequency. The values presented here are calculated for one counter electrode. BFCC = binder free carbon composite, PCC = PEDOT–carbon composite, BCC = binder carbon composite (Reproduced from publication 4 with permission from PCCP Owner Societies).

The EIS response for any type of carbon composite for instance e.g. PEDOT carbon composite (PCC) based DSC is slightly different compared to platinum counter electrode based DSC where typically a large semicircle appears (for instance in Publication 4 the PCC CE on each substrate i.e. glass = 3.8 Ωcm^2, ITO-PET = 4.5 Ωcm^2 and ITO-PEN = 4.1 Ωcm^2) due to the overlapping of R_{CT} and R_{REC} response at lower frequency range (~10-20 Hz Fig.11 a-b). Hence it is difficult to estimate the exact value of R_{CT} from Fig. 11 (a) in case of a porous carbon based CE. The same response of carbon gel catalyst layer can be seen in

Figure 10 a-b. One way to estimate R_{CT} is to subtract R_{REC} from the value since the PE geometry in each type of DSC was the same (0.4 cm^2).
One very small semicircle, which is adjacent to the large semi-circle can also be identified in each EIS spectrum of carbon composite (Figure 10 and 11 a i.e. Figure 11 a: Glass-PCC = 1.3 Ωcm^2, ITOPET-PCC = 2.0 Ωcm^2, ITOPEN-PCC = 1.5 Ωcm^2) which appears at very high frequency ~ 10 kHz) and is associated with a second Nernst diffusion impedance resulted from diffusion through the pores of carbon composite [58]. The values of these extra semicircles were added to the charge transfer resistance to get the total charge transfer resistance ($R_{CE\text{-}total}$).

The argument was verified by making CE-CE cell of each type of carbon composite reported in Publication 4. The advantage of making a symmetrical cell is that it eliminates all the possible responses from the PEs. In Figure 12b, all carbon composites exhibited 2 peaks which were already expected; one in the lower (10–100 Hz) and the other in the higher frequency range (100 kHz). These are associated with the charge transfer resistance and the in-pore diffusion resistance respectively (Figure 12 b). This also certifies our earlier observation about the overlapping PE and CE semicircles in the DSCs, meaning that the peak must be associated with the porous carbon CE as here we have no PE. The thermally platinized glass CE–CE cell exhibited two frequency peaks at similar positions than in the complete DSC corresponding to recombination resistance (R_{REC}) and diffusion resistance (R_D).

It should be noted that the tested composites in Publication 4 exhibited lower or comparable charge transfer values than the carbon gel catalyst layer. The only difference between the carbon gel catalyst and other composites was the ball milling step (each composite was milled for two hours) that was performed during the preparation of BFCC, BCC and PEDOT carbon composites. The ball milling step is well-known in the formulation of screen printable pastes for this technology. We assumed here that this ball milling step increased the surface area of the carbon composites nanoparticles, i.e. more catalytic sites were available for the tri-iodide reduction as compared with carbon gel catalyst layer.

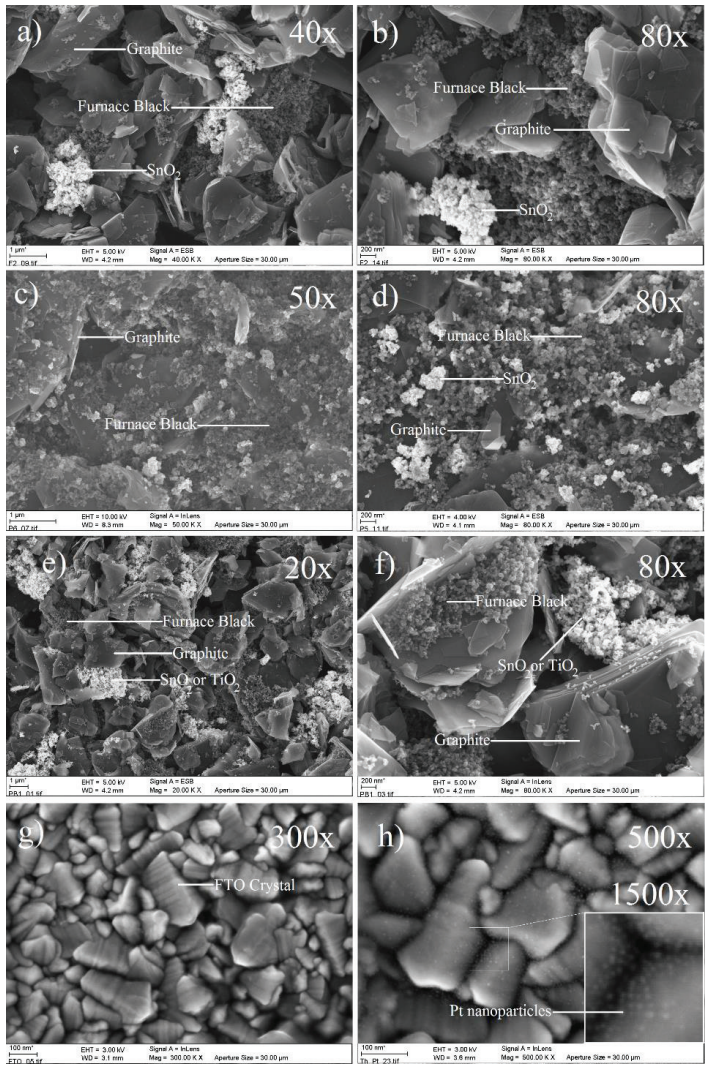

Figure 13. SEM images of different carbon composites: (a-b) BFCC, (c and d) PCC, (e and f) BCC, (g) bare FTO-glass, (h) thermally platinized CE. BCC = binder carbon composite, PCC = PEDOT–carbon composite, BFCC = binder free carbon composite. X stands for magnification. (Reproduced from publication 4 with permission from PCCP Owner Societies).

The SEM images in this study confirms the perception about the ball milling by revealing highly porous structures in case of each composite compared with platinum nano particles (Figure 13 a-h). With this ball mill step, the PEDOT based carbon composite outperformed the catalytic activity of reference thermal platinum counter electrode in the complete device and showed very low R_{CT} values both on ITO-PEN (1.8 Ωcm^2) and ITO-PET (2.7 Ωcm^2) compared to R_{CT} value (4.9 Ωcm^2) of thermally platinized counter electrodes (See Table 3 of Publication 4). Also in the CE-CE configurations, all types of composites exhibited very

low R_{CT} values (3-3.9 Ωcm^2) which was lower/equal the R_{CT} value of platinum CE-CE cell.

Hence we successfully tested all these composites of carbon as an alternative catalyst layers to expensive Pt catalyst in the DSC. Some of the composites such as the carbon gel or PEDOT carbon composite showed good mechanical stabilities over plastics, but they still require a highly conductive under layer which was ITO (Indium doped tin oxide) over plastics and FTO (Fluorine doped tin oxide) on glass. These materials are realized as scarce and expensive components in the DSC. If these carbon composites could be engineered with other abundantly available conducting materials such as carbon, this could also be a viable solution to address the cost issues.

4.4.3 A novel SWCNT coated flexible PVC counter electrode for DSC (Publication 5)

As discussed in the earlier sections, the flexible polymer substrates for DSC utilize transparent conducting oxide (TCO) and more precisely indium doped tin oxide (ITO) layer that has been realized as a scarce and one of the most expensive components of DSC. Additionally the sheet resistance of the ITO layers varies from 5 to 60 Ω/Square i.e. Ω/Sq which is sufficient for the DSC application. Although inexpensive metallic substrates provide an alternative solution, the corrosion of the metallic sheets in the electrolyte solution makes it impractical to properly address the problem. One probable possibility is a combination of a nonmetallic conductor such as carbon nanotubes over a polymer substrate that can potentially give the same alternatives to non-transparent metals by eliminating the chances of corrosion. Based on our experience from our studies, the major challenge associated with carbon materials is robust adhesion like with ITO over plastics that does not come out easily. Also the critical 'sintering' step cannot be applied over plastics due to their temperature limitations (max. 150 °C). The challenge was to develop an ink formulation of carbon nanotubes that could produce high conductivity with the low temperature treatments required for DSC. In our earlier studies we presented metal free counter electrodes that were constructed by depositing the carbon nanotubes via dry transfer process [47]. This process is slow and it takes hours to collect the nanotubes on filter. Secondly

the collected nanotubes on filter were stamped on PET polymer mechanically which does not give sufficient adhesion on the substrates.

Keeping these problems in mind, an aqueous single walled carbon nanotubes (SWCNT) ink was prepared that was spread on commonly available PVC polymer through a pipette and was then placed on a preheated hotplate at 100-120 °C. Upon the drying of the solvent (water) over hotplate (within 5 minutes), highly conductive CNT pattern were obtained as shown in Figure 14 (a-c) and the nonconductive PVC polymer sheet was transformed into a highly conductive substrate. The mechanical adhesion of the obtained CNT patterns was tested with 60 times bending test over different radii as well as with tape adhesion test. The results are summarized in Figure 15 (a-d) and Figure 16 (a-b). In short the CNT over PVC substrate exhibited remarkable adhesion and the sheet resistance (R_{SH}) was hardly changed upon each stress as shown in Figures 15 and 16. Due to this high conductivity and good mechanical stability, this SWCNT loaded PVC substrate was used as a counter electrode in dye sensitized solar cells by spin coating a catalyst layer (PEDOT-TsO), as we already knew from our past experiments that CNTs alone were not catalytic enough.

The photovoltaic and electrochemical performance of the fabricated cells were recorded under 1000 W/m^2 light intensity of an artificial solar simulator equivalent to 1 Sun light intensity. In these measurements the cells fabricated with PVC/SWCNT/PEDOT counter electrodes exhibited 5% efficiency compared to 5.2% percent reference platinum counter electrode cells. The reason for slightly lower performance was a low fill factor due to higher series resistance (R_S). The higher series resistance of PVC counter electrodes is understandable because of the surfactant that was added in the ink solution and cannot be removed due to restrictions of the temperature. However, this factor can easily be optimized by adjusting the surfactant concentrations. Moreover the PVC counter electrodes exhibited very low charge transfer resistance ($R_{CT} = 1.4 \pm 0.7$ Ωcm^2) compared to 2.2 ± 0.5 Ωcm^2 of the reference platinum counter electrode based DSCs. This successful demonstration of PVC/SWCNT/PEDOT counter electrode offers an alternative solution for metals in the DSC. Although the experiment was performed on PVC polymer it can also be potentially performed on PET polymer foil.

Figure (14 a-c): Demonstration of ink deposition a) patterning of the substrate, b) application of ink and evaporation of solvent at 120 °C in 5 minutes c) SWCNT patterns (Copyright Wiley-VCH Verlag GmbH & Co. KGaA. Reproduced from Publication 5 with permission).

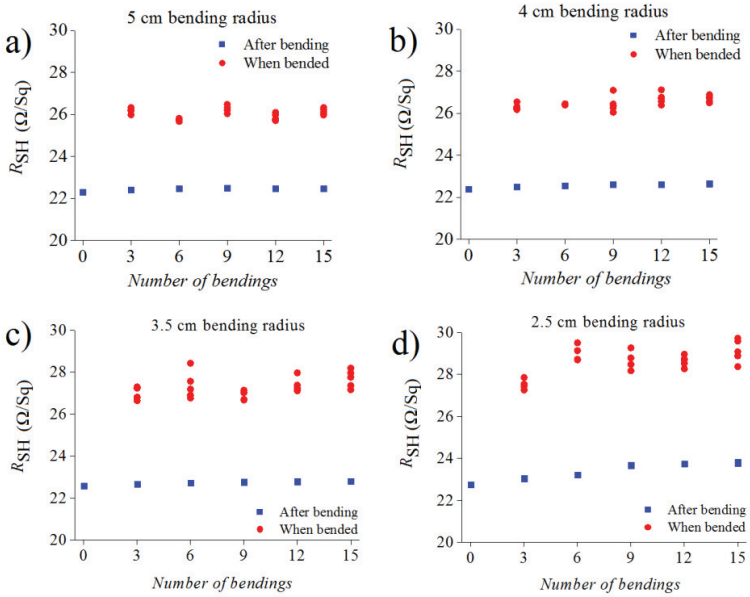

Figure 15 (a-d): Bending test of deposited SWCNT ink over PVC substrate with different bending radius. The first blue square in each figure represents the initial sheet resistance before bending. (Copyright Wiley-VCH Verlag GmbH & Co. KGaA. Reproduced from Publication 5 with permission).

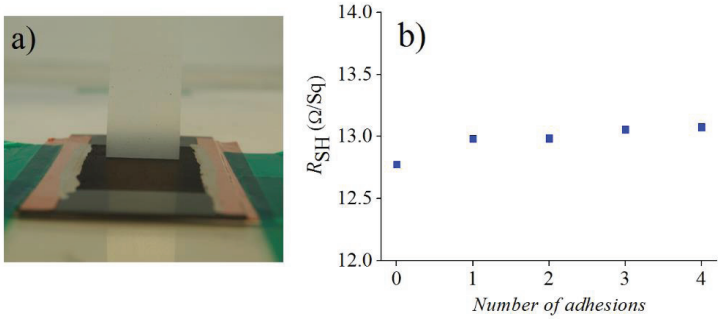

Figure 16 (a-b): Tape adhesion test results of deposited single walled carbon nanotube ink on PVC sheet. a) Pressure sensitive tape pulling at 90°, b) Sheet resistance versus number of times tape applied (Copyright Wiley-VCH Verlag GmbH & Co. KGaA. Reproduced from Publication 5 with permission).

4.4.4 Spatial variations in large area dye solar cells and their optimization via electrolyte filling process (Publication 6)

The purpose of this study was to optimize/minimize the spatial variations that appears in a large area cell by optimizing the electrolyte filling process. The spatial variations in large area DSC is well-known and has also been reported in our previous studies [59-61]. It was found that the conventional electrolyte filling process exhibits non-uniform distributions of its components that affects the overall performance precisely in the large area DSC. To study these variations, we designed a segmented cell that was consisted of 8 individual cells (segments) electrically isolated from each other via scribing the TCO layer but were sharing the same electrolyte as shown in Figure 17. First the conventional one-way electrolyte filling step was performed by injecting the electrolyte from holes A to B and the *IV* measurements were recorded. After that all the electrolyte was sucked through a suction pump and new electrolyte was once again injected from holes B to A and the *IV* measurements were recorded. We called this process two-way filling. The trends of photovoltaic parameters are shown in Figure 18 (a-d).

For the one-way filling, a slight decrease in J_{SC} values from segment 1 to 8 as well as a continuous decrease in the V_{OC} was observed which resulted in a 20% loss in the efficiency throughout 8 segments (Figure 18 a-b). These observations were in complete agreement to our previous reported studies which confirms the hypotheses about the electrolyte distribution since the only variable was the electrolytes and its components. The fact here is that the mesoporous TiO_2 layer acts here as a molecular filter and caused the uneven distribution of the electrolyte components [60]. The NMBI in our previous reports among the other electrolyte components was identified as the non-uniformly distributed component as its higher concentration was found near the filling holes during this traditional one-way filling [60].

In order to compensate this spatial distribution effect, a new two-way filling was introduced which helped in balancing the performance of the cell channel from both ends. The two-way filling confirmed the hypothesis and J_{SC} was improved by 19-38% and a major enhancement (4-10%) in V_{OC} was obtained (Figure 18 a-b). As a result, the efficiencies improved by 24-55% throughout the segments

(Figure 18 d). These improvements were obtained due to reduction of spatial distributions of the electrolyte components throughout the segmented channel. Additionally the combined photovoltaic response of all parallel connected 8 cells was also recorded with both types of filling methods. With the one way filling an efficiency of 3.4% was obtained whereas the two-way filling resulted in an overall efficiency of 4.8% which is 42% higher than obtained with the one-way filling method.

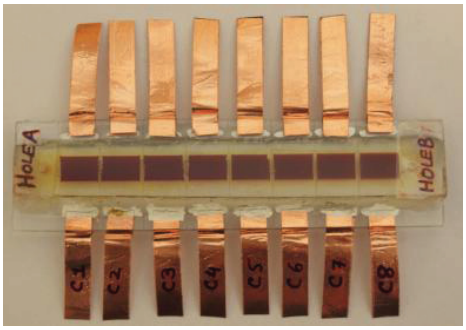

Figure 17: A segmented cell with eight segments (counted as 1-8 from holes A to B) (Reprinted from Publication 6 with the permission of EU PVSEC Proceedings).

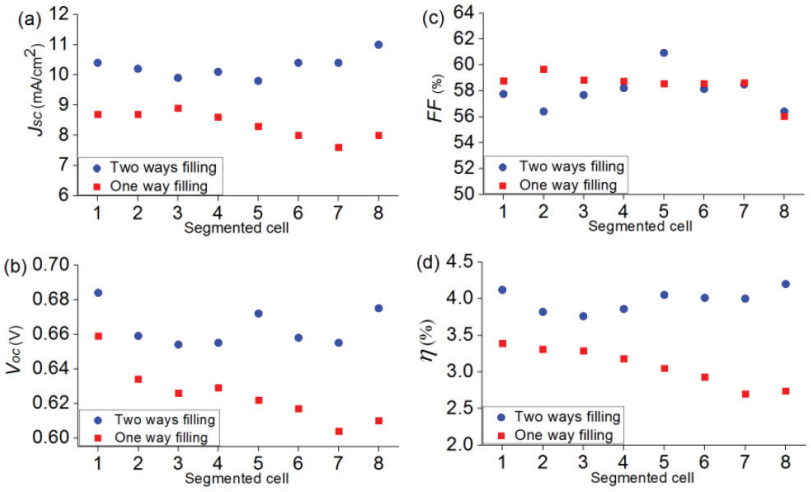

Figure 18. Trends of one way and two ways electrolyte filling of the segmented cells (a) J_{SC} (b) V_{OC} (c) *FF* and (d) Efficiency. (Reprinted from Publication 6 with the permission of EU PVSEC Proceedings).

From these results three different types of large area stripes cells were fabricated: as reference a completely rigid cell (Glass based PE and Glass based Platinum

counter electrodes), semi flexible (Titanium foil based PE and Glass based Platinum counter electrodes) and completely flexible (Titanium foil based PE and Chemically platinized CE on ITO PEN). The completely rigid reference cell exhibited an overall efficiency of 4.1% whereas the reverse illuminated semi flexible cell showed 3.9% efficiency. The efficiency was dropped down to 3.4% with fully flexible (Ti_{PE}-PEN_{CE}) which was slightly (20%) lower compared to the reference cell.

To conclude, the traditional electrolyte flow filling method resulting the non-homogeneous distribution of its components which consequently exhibit spatial variations in the overall performance of large area DSC. Although we are able to reduce the effect of this non-homogeneous distribution with the new two ways filling method, however, some other alternative procedure needs to be explored. A probable solution could be the printing of electrolyte formulation as proposed in Publication 1 which may introduce more homogeneous distribution of the electrolyte components and might be able to resolve the problem.

5. Conclusion and summary

This thesis provides a technical overview regarding the critical steps of dye sensitized solar cells on alternative substrates (mainly on plastic substrates) to pave the way towards low-cost DSCs The unique thing about the DSC is that it offers numerous material combinations of which some were tested in this research work.

Another aim was to develop low temperature inks/paste that could also be realized for high volume manufacturing processes. The thesis also provides some details regarding the mechanical stability of the materials that were deposited through a low-temperature route that is rarely reported in the literature.

We systematically reviewed the state of the art of DSC technology and then constructed a systematic comparison of different types of important counter electrode material which were identified during the review. This study was performed by keeping the same PE geometry which gave more precise results/conclusions about their characteristics. Despite of higher costs, the chemically deposited platinum catalyst still looks best among the tested semitransparent catalyst layers and exhibited the best performance in terms of efficiency (3.1%) when realized for the reverse illuminated type of flexible DSC combinations in comparison with electrochemical Pt (2.6%) and PEDOT-TsO (2.2%). Also the catalytic activity of chemically platinized layer remained superior (R_{CT} = 3.7 Ωcm^2) among all the tested low temperature catalysts (R_{CT} = 12 Ωcm^2 for electrochemical platinization, R_{CT} = 5.8 Ωcm^2 for PEDOT-TsO and R_{CT} = 11 Ωcm^2 for Carbon gel catalyst layer). The carbon gel catalyst layer showed comparable performance with commercially available high temperature carbon paste, but its charge transfer resistance needs to be decreased. The adhesion of the PEDOT-TsO catalyst was found problematic requiring special treatment such as a separator layer to avoid the problem.

We systematically studied different low temperature carbon composites as alternative catalyst materials for DSC. Mechanical stability tests to verify their adhesive properties were also performed which is very important in order to develop low-temperature inks/pastes based flexible DSC modules. The key findings were

improved R_{CT} values (3-3.9 Ωcm^2) compared to reference Pt counter electrode (4 Ωcm^2). One of these composites (BCC=binder enriched carbon composite) achieved 6% overall efficiency compared to 7% of the reference Pt counter electrode based DSC. Good mechanical testing stability was achieved on all substrates (FTO Glass, ITO-PEN and ITO-PET) with PEDOT-carbon composite catalyst layers.

To avoid an expensive and scarce conducting ITO layer, we developed an aqueous ink of single walled carbon nanotubes (SWCNT) and implemented it successfully on a non-metallic PVC polymer sheet. The highly conductive patterns of SWCNT showed remarkable elastic and adhesion capability and exhibited fractional changes in the sheet resistance of ~ 8% and 3% when subjected to harsh bending and tape tests respectively. The photovoltaic and electrochemical performances of the CNT coated PVC counter electrode was similar (5% and R_{CT} = 2.7 Ωcm^2) as in the reference DSC (5.2% and R_{CT} = 2.2 Ωcm^2). These key findings can also be realized as an alternative solution to the corrosion-sensitive metallic flexible sheets.

Finally we also highlighted the spatial distribution losses in a large area DSC and presented a solution via a two-way filling method to minimize the effect of unevenly distributed electrolyte components. The overall performance (cell efficiency) of the segmented cell was improved up to 42% when the spatial losses were suppressed with the two-ways filling method. We also recommend the electrolyte printing as more practical solution to address the spatial losses where homogeneous distribution of the electrolyte components may be expected than the conventional electrolyte filling method. Also the careful optimization of electrolyte composition is also recommended.

This thesis highlights the critical issues in the realization of fabricating the flexible DSCs and presents the characteristics and potential of the different low cost materials in several ways. At the moment the prices of some materials such as single walled carbon nanotubes are still high, but the learning curves of matured technologies implies that a fall in prices of these materials is expected. In short the key issues in fabrication of flexible DSC require precise solutions to speed up the industrialization of DSC. Also the stability of flexible DSC which was

not the topic for this thesis is an important question. Especially, the usage of non-volatile liquid solvent such as 3-Methoxypropionitrile is one of the critical requirements for durable flexible DSC. The flexible polymer based PE is still a challenge for the front side illumination due to difficulties in realizing high efficiency photoelectrodes with low temperature processing. As well as penetration of moisture and oxygen in flexible dye solar modules/cells has been reported in several publications. All these problem raise questions for the development of robust materials that could be able to resist harsh conditions.

The focus of the future research could be the development of a highly conductive PET polymer foil by utilizing the SWCNT ink that could be used as a counter electrode which is a more practical solution for the fabrication of flexible DSC as compare to PVC polymer based counter electrode. Such flexible conductive PET foil could then be equipped with the low-temperature TiO_2 flexible PE to get a fully flexible DSC.

7. References

[1] International Energy Outlook 2013.

[2] Global market outlook for Photovoltaics 2013-2017.

[3] Experience Curves for Energy Technology Policy, IEA, 2000,

[4] Solar Photovoltaics. A technologist's view. http://www.carbonin-sights.org/?p=818.

[5] J. H. Park, Y. Jun, H. Yun, S. Lee, M. G. Kang, *J. Electrochem. Soc* **2008**, 155, F145.

[6] A. Yella, H. W. Lee, H. N. Tsao, C. Yi, A. K. Chandiran, M. K. Nazeeruddin, E. W. G. Diau, C. Y. Yeh, S. M. Zakeeruddin, M. Grätzel, *Science*, **2011**, 334, 629.

[7] M. A. Green, K. Emery, Y. Hishikawa, W. Warta, E. D. Dunlop, *Prog. Photovolt: Res. Appl*, **2014**, 22, 1.

[8] http://www.dyesol.com/

[9] J. Kalowekamo, E. Baker, *Solar Energy*, **2009**, 831224.

[10] http://www.g24i.com/

[11] M. I. Asghar, K. Miettunen, J. Halme, P. Vahermaa, M. Toivola and K. Aitola, *Energy. Environ. Sci*, **2010**, 3, 418.

[12] J. Chen, B. Li, J. Zheng, J. Zhao, H. Jing, Z. Zhu, *Electrochim. Acta*, **2011**, 56, 4624.

[13] J. Chen, K. Li, Y. Luo, X. Guo, D. Li, M. Deng, S. Huang, Q. Meng, *Carbon*, **2009**, 47, 2704.

[14] G. Veerappan, K. Bojan, S. Rhee, *Renew. Energy*, **2012**, 41, 383.

[15] M. Ikegami, J. Suzuki, K. Teshima, M. Kawaraya, T. Miyasaka, *Sol. Energy. Mater. Sol. Cells*, **2009**, 93, 836.

[16] K. M. Lee, W. H. Chiu, M. D. Lu, W. F. Hsieh, *J. Power. Sources*, **2011**, 15 8897.

[17] J. Halme, P. Vahermaa, K. Miettunen, P. Lund, *Adv. Energy. Mater,* **2010**, 22, E210.

[18] G. Hashmi, K. Miettunen, J. Halme, I. Asghar, H. Vahlman, T. Saukkonen, Z. Huaijin, P. Lund, *J. Elect. Chem. Soc,* **2012,** 159, H656.

[19] S. G. Hashmi, J. Halme, T. Saukkonen, E. Rautama, P. Lund, *Phys. Chem. Chem. Phys,* **2013**, *15*, 17689.

[20] a) Association connecting electronics industries, Tape testing methods manual, http://www.ipc.org/TM/2.4.1E.pdf; b) Peel adhesion of pressure sensitive tape, **2007**, http://www.pstc.org/files/public/101.pdf

[21] B. Wang, L. L. Kerr, *Sol. Energy. Mat. Sol. Cells,* **2011**, 95, 2531.

[22] F. C. Krebs, T. Tromholt, M. Jorgensen, *Nanoscale,* **2010**, 2, 873.

[23] Y. Wang, H. Yang, Y. Liu, H. Wang, H. Shen, J. Yan et al. *Prog. Photovolt*. **2010**, 18, 285.

[24] http://www.alibaba.com/productgs/260984640/Pure_and_alloy_titanium_foil_minimum.html

[25] K. Zweibel, *Sol. Energy. Mater. Sol. Cells,* **2000,** 63, 375.

[26] http://www.alibaba.com/productgs/309148412/Household_aluminum_foil.html

[27] J. M. Kroon, N. J. Bakker, H. J. P. Smit, P. Liska, K. R. Thampi, P. Wang et al. *Prog. Photovolt,* **2007**, 15, 1.

[28] http://www.sigmaaldrich.com/catalog/product/aldrich/520896?lang=fi&region=FI

[29] http://www.sigmaaldrich.com/catalog/search?interface=All&term=Indium%20tin%20oxide&lang=fi&region=FI&focus=product&N=0+220003048+219853114+219853286

[30] http://www.sigmaaldrich.com/catalog/product/aldrich/332461?lang=fi&region=FI

[31] N. Tanabe, Recent progress in DSC module panel development at Fujikura Ltd. *DSC-IC 2010* **2010**.

[32] X. Fang, T. Ma, M. Akiyama, G. Guan, S. Tsunematsu, E. Abe, *Thin*. *Solid*. *Films*, **2005,** 472, 242.

[33] T. Yamaguchi., N. Tobe, D. Matsumoto, T. Nagai, H.Arakawa. *Sol*. *Energy*. *Mater*. *Sol*. *Cells*, **2010**, 94, 812.

[34] J. Scheirs, L. Gardette. *Polym*. *Degrad. Stab*, **1997**, 56, 339.

[35] K. F. Jensen (PhD thesis: Performance comparison of a dye-sensitized and a silicon solar cell under idealized and outdoor Conditions).

[36] http://www.sony.net/SonyInfo/csr/SonyEnvironment/technology/solar_cells.html

[37] M. Duerr, A. Schmid, M. Obermaier, S. Rosselli, A. Yasuda, G. Nelles, *Nat. Mater*, **2005**, 4, 607.

[38] H. C. Weerasinghe, P. M. Sirimanne, G. P. Simon and Y. B. Cheng, *Prog. Photovolt. Res. Appl*, **2012**, 20, 321.

[39] H. C. Weerasinghe, P. M. Sirimanne, G. P. Simon, Y. B. Cheng, *J. Photochem. Photobio. A: Chem*, **2009**, 206, 64.

[40] D. Zhang, T. Yoshida, K. Furuta, H. Minoura, *J. Photochem. Photobio. A,* **2004**,164, 159.

[41] T. N. Murakami, Y. Kijitori, N. Kawashima, T. Miyasaka, *Chem. Lett*, **2003**, 32, 1076.

[42] H. Pan, S. H. Ko, N. Misra, C. P. Grigoropoulos, Appl. *Phys. Lett,* **2009**, 94, 071117/1.

[43] S. Ito, N. L. Ha, G. Rothenberger, P. Liska, P. Comte, S. Zakeeruddin, P. Pechy, M. Nazeeruddin, and M. Gratzel, *Chem. Commun*, **2006**, 38, 4004

[44] T. Miyasaka, M Ikegami, Y. Kijitori. *J. Electrochem. Soc*, **2007,** 154, A455.

[45] H. Lindstrom, A. Holmberg, E. Magnusson, L. Malmqvist, A. Hagfeldt, *J. Photochem. Photobiol. A* **2001**, 145, 107.

[46] J. M. Pringle, V. Armel, M. Forsyth, D. R. MacFarlane, *Aust. J. Chem,* **2009**, 62, 348.

[47] K. Aitola, M. Borghei, A. Kaskela, E. Kemppainen, A. G. Nasibulin, E. I. Kauppinen, P. D. Lund, V. Ruiz and J. Halme, *J. Electroanal. Chem*, **2012**, 683, 70.

[48] A. Hauch, A. Georg. *Electrochim. Acta*, **2001**, 46, 3457.

[49] X. Fang, T. Ma, G. Guan, M. Akiyama, T, Kida, E. Abe. *J. Electroanal. Chem*, **2004**, 570, 257.

[50] Y. Saito, T. Kitamura, Y. Wada, S. Yanagida, *Chem. Lett*, **2002**, 10, 1060.

[51] T. Muto, M. Ikegami, K. Kobayashi, T. Miyasaka, *Chem. Lett*, **2007**, 36, 804.

[52] S. Ahmad, J. Yum, Z. Xianxi, M. Gratzel, H. Butt, M. K. Nazeeruddin, *J. Mater. Chem*, **2010**, 20, 1654.

[53] D. Kuang, C. Klein, Z. Zhang, S. Ito, J. Moser, S. M. Zakeeruddin, M. Gratzel, Small, **2007**, 3, 2094.

[54] N. Jiang, T. Sumitomo, Lee, A. Pellaroque, O. Bellon, D. Milliken, H. Desilvestro, *Sol. Energy Mater. Sol. Cells*, **2013**, 119, 36.

[55] S. M. Zakeeruddin, M. Gratzel, *Adv. Funct. Mater*, **2009**, 19, 2187.

[56] N. Kato, Y. Takeda, K. Higuchi, A. Takeichi, E. Sudo, H. Tanaka, et al. *Sol. Energy Mater. Sol. Cells*, **2009**, 93, 893–897.

[57] H. Lindstrom, A. Holmberg, E. Magnusson, S. Lindquist, L. Malmqvist, A. Hagfeldt, *Nano. Lett* **2001**, 1, 97.

[58] J. D. Roy-Mayhew, D. J. Bozym, C. Punckt and I. A. Aksay, *ACS. Nano*, **2010**, 4, 6203.

[59] K. Miettunen, J. Halme, P. Lund, *Electrochem. Comm*, **2009**, 11, 25.

[60] K. Miettunen, M. I. Asghar, S. Mastroianni, J. Halme, P. R. F. Barnes, E. Rikkinen, B. C. Regan, P. Lund, *J. Electroanal. Chem*, **2012**, 664, 63.

[61] K. Miettunen, P. R. F. Barnes, X. Li, C. H. Law, B. C. Regan, , *J. Electro-anal. Chem*, **2012**, 677, 41.

Take the attitude of a student, never be too big to ask questions, never know too much to learn something new.

Og Mandino

Aalto-DD 41/2014

ISBN 978-952-60-5625-8
ISBN 978-952-60-5626-5 (pdf)
ISSN-L 1799-4934
ISSN 1799-4934
ISSN 1799-4942 (pdf)

Aalto University
School of Science
Department of Applied Physics
www.aalto.fi

BUSINESS + ECONOMY

ART + DESIGN + ARCHITECTURE

SCIENCE + TECHNOLOGY

CROSSOVER

DOCTORAL DISSERTATIONS